Research in Astron. Astrophys. **2013** Vol. **13** No. **4**, 490–500
http://www.raa-journal.org *http://www.iop.org/journals/raa*

***R**esearch in*
***A**stronomy and*
***A**strophysics*

Atmospheric extinction coefficients and night sky brightness at the Xuyi Observation Station *

Hui-Hua Zhang[1], Xiao-Wei Liu[1,2], Hai-Bo Yuan[2,†], Hai-Bin Zhao[3], Jin-Sheng Yao[3], Hua-Wei Zhang[1] and Mao-Sheng Xiang[1]

[1] Department of Astronomy, Peking University, Beijing 100871, China; *x.liu@pku.edu.cn*
[2] Kavli Institute for Astronomy and Astrophysics, Peking University, Beijing 100871, China
[3] Purple Mountain Observatory, Chinese Academy of Sciences, Nanjing 210008, China

Received 2012 August 13; accepted 2012 November 9

Abstract We present measurements of the optical broadband atmospheric extinction coefficients and the night sky brightness at the Xuyi Observation Station of Purple Mountain Observatory. The measurements are based on CCD imaging data taken in the Sloan Digital Sky Survey's g, r and i bands with the Xuyi 1.04/1.20 m Schmidt Telescope for the Xuyi Schmidt Telescope Photometric Survey of the Galactic Anti-center (XSTPS-GAC), the photometric part of the Digital Sky Survey of the Galactic Anti-center (DSS-GAC). The data were collected during more than 140 winter nights from 2009 to 2011. We find that the atmospheric extinction coefficients for the g, r and i bands are 0.69, 0.55 and 0.38 mag/airmass, respectively, based on observations taken on several photometric nights. The night sky brightness determined from images with good quality has median values of 21.7, 20.8 and 20.0 mag arcsec^{-2} and reaches 22.1, 21.2 and 20.4 mag arcsec^{-2} under the best observing conditions for the g, r and i bands, respectively. The relatively large extinction coefficients compared with other good astronomical observing sites are mainly due to the relatively low elevation (i.e. 180 m) and high humidity at the station.

Key words: techniques: astronomical observing sites — atmospheric extinction coefficients — night sky brightness

1 INTRODUCTION

The atmospheric extinction coefficients and night sky brightness are key parameters characterizing the quality of an astronomical observational site, in addition to the seeing and the number of clear nights. The atmospheric extinction is the brightness reduction of celestial objects as their light passes through the Earth's atmosphere. Parrao & Schuster (2003) points out that precise atmospheric extinction determinations are needed not only for stellar photometry but also for any sort of photometry, spectroscopy, spectrophotometry and imaging whenever accurate, absolute and well-calibrated photometric measurements are required for the derivation of physical parameters in the studies of

∗ Supported by the National Natural Science Foundation of China.
† LAMOST Fellow.

galaxies, nebulae, planets, and so forth. Precise determinations of the atmospheric extinction ultimately determine the scientific value of the telescopic data. The night sky brightness is caused by scattered starlight, airglow, zodiacal light and artificial light pollution from nearby cities. They are the main sources of noise affecting ground-based astronomical observations. The night sky brightness limits the detection depth of a telescope – the lower the night sky brightness, the fainter the stars that can be detected and the more astronomical information that can be collected.

All good astronomical sites around the world have been subject to comprehensive studies of their atmospheric extinction properties and night sky brightness measurements. For example, Krisciunas et al. (1987) and Krisciunas (1990) studied the Mauna Kea site, the location of the Canada France Hawaii Telescope (CFHT), the Keck 1 & 2, and the Subaru telescopes as well as the future Thirty Meter Telescope (TMT) which is under development. Burki et al. (1995) and Mattila et al. (1996) studied the La Silla site, and their results were used to derive the characteristics of the Las Campanas site that hosts the Giant Magellan Telescope (GMT). Tokovinin & Travouillon (2006) modeled the optical atmospheric turbulence of the Cerro Pachon site which has been selected for the Large Synoptic Survey Telescope (LSST). The atmospheric extinction and night sky brightness of La Palma, site of the Gran Telescopio Canarias (GTC) and of a number of smaller telescopes, have been studied by García-Gil et al. (2010) and Benn & Ellison (1998), respectively. Patat et al. (2011) measured the atmospheric extinction of the Cerro Paranal, site of the Very Large Telescope (VLT). Parrao et al. (2003) studied the atmospheric extinction of the San Pedro Mártir (SPM) site.

In those studies mentioned above, different methods of measuring the atmospheric extinction and night sky brightness have been proposed and the results are discussed in terms of relavent factors such as aerosols, water vapor content, airglow, zodiacal light and light pollution. Krisciunas (1990) and Krisciunas (1997) also studied and confirmed the effects of solar activities on night sky measurements. Krisciunas & Schaefer (1991) constructed a model for the brightness of moonlight and Garstang (1989) investigated the sky brightness caused by sky glow. Hogg et al. (2001) studied the atmospheric extinction of Apache Point Observatory and described a near real-time extinction monitoring instrument that has significantly improved the photometric calibration of the Sloan Digital Sky Survey (SDSS). Burke et al. (2010) proposed a method for precise determinations of the atmospheric extinction by studying the absorption signatures of different atmospheric constituents, which might be applied to future ground-based surveys such as the LSST. Real-time, accurate measurements of the night sky's atmospheric properties will be of increasing importance for future ground-based surveys.

The Digital Sky Survey of the Galactic Anti-center (DSS-GAC; Liu et al. 2013, in preparation), is a spectroscopic and photometric survey targeting millions of stars distributed in a contiguous sky area of about 3500 deg^2 centered on the Galactic Anti-center. The spectroscopic component of the DSS-GAC, the Guo Shou Jing Telescope (LAMOST) Spectroscopic Survey of the Galactic Anti-center (GSJTSS-GAC), will secure optical spectra for a statistically complete sample of over three million stars of all colors and spectral types, whereas its photometric component, the Xuyi Schmidt Telescope Photometric Survey of the Galactic Anti-center (XSTPS-GAC) surveyed the area in the SDSS g, r and i bands with a wide field CCD using the Xuyi 1.04/1.20 m Schmidt Telescope in order to provide the spectroscopic target input catalogs for the GSJTSS-GAC. XSTPS-GAC was initiated in October 2009 and completed in March 2011. In total, over 20 000 images have been collected over more than 140 nights. The survey reached a limiting magnitude of 19 (10σ) in all three bands. Approximately 100 million stars have been detected and cataloged in the i band, and approximately half that number in the g band.

The Xuyi Schmidt Telescope is located on a small hill about 35 km from Xuyi town in the middle-east of China with an elevation of about 180 m above sea level, similar to that of Fowler's Gap in Australia, a potential site for a Cherenkov telescope (Hampf et al. 2011). The atmospheric extinction and night sky brightness of the Xinglong station, where LAMOST is located, have been studied by Yan et al. (2000), Liu et al. (2003) and Yao et al. (2012), respectively. In this work, we

present measurements of the atmospheric extinction coefficients and night sky brightness of Xuyi Station using the data collected from the XSTPS-GAC. The data have been analyzed using the traditional methods. The telescope's characteristics and the basic data reduction steps are briefly outlined in Section 2. Section 3 presents measurements of the atmospheric extinction coefficients. In Section 4, we describe statistical measurements of the night sky brightness and discuss the potential effects of the Moon phase/brightness and the contribution of the Galactic disk to brightness measurements of the night sky. Finally, the conclusions follow in Section 5.

2 OBSERVATIONS AND DATA REDUCTION

The Xuyi Schmidt Telescope is a traditional ground-based refractive-reflective telescope with a diameter of 1.04/1.20 m. It is equipped with a thinned 4096×4096 CCD camera, yielding a $1.94^\circ \times 1.94^\circ$ effective field-of-view (FoV) at a sampling of $1.705''$ per pixel projected on the sky. The CCD quantum efficiency, at the cooled working temperature of -103.45°C, has a peak value of 90 percent in the blue and remains above 70 percent even to wavelengths as long as 8000 Å. The XSTPS-GAC was carried out with the SDSS g, r and i filters. The current work presents measurements of the Xuyi atmospheric extinction coefficients and the night sky brightness in the three SDSS filters based on the images collected for the XSTPS-GAC.

The XSTPS-GAC images cover a total sky area of 6000 deg^2 centered on the Galactic Anticenter, from $3h$ to $9h$ in right ascension (RA) and from -10° to $+60^\circ$ in declination (DEC), plus an extension of about 900 deg^2 in the area toward M31/M33. Most observations were carried out in dark or grey nights with good photometric quality. A small fraction of the observations were taken under bright lunar conditions and in those cases, the angular distances between the field centers and the Moon were kept at greater than 60 °. An integration time of 90 s was used for all exposures, with a readout time of approximately 43 s in dual-channel slow readout mode. The field center stepped in RA by half the FoV (i.e. 0.97 °), leading to two exposures for a given point of the sky. Two stripes representing scans of adjacent declinations overlapped by approximately 0.04 °. Normally, two stripes of fields from adjacent declinations were scanned in a given night. The stripes crossed the Galactic disk from south to north, a fact that we have found useful to quantify the effects of the bright Galactic disk for measurement of night sky brightness. With this specific combination of integration time and scanning strategy, the movement of the telescope pointing was minimized in a given night, ensuring maximum uniformity of the survey. To facilitate the global flux calibration, a few "Z" stripes of fields, that straddled regions between the fields of "normal" stripes, were also observed. Finally, in the course of the survey, in order to measure the atmospheric extinction coefficients, several photometric nights were selected and used to carry out repeated exposures of a few preselected fixed fields at different zenith distances, with a time interval between exposures of half an hour.

Each raw image was bias-subtracted and flat-fielded, using a super-sky-flat (SSF) generated from all frames taken with the same filter in the same night. There was interference fringing in the i band images. However, the fringing pattern was found to be stable for a given night, and thus could be effectively removed by SSF fielding. Aperture and point spread function (PSF) photometry was then performed using a package developed by the Beijing-Arizona-Taiwan-Connecticut (BATC) Sky Survey (Fan et al. 1996; Zhou et al. 2001) based on the widely used package of DAOPHOT (Stetson 1987). The astrometry was initially calibrated with the GSC2.0 (Bucciarelli et al. 2001) reference catalog, and then the plate distortion was corrected using a 30-parameter solution based on the PPMXL (Roeser et al. 2010) reference catalog, yielding an accuracy of about $0.1''$ (Zhang et al., in preparation). An Ubercal (Padmanabhan et al. 2008) photometric calibration was achieved by calibrating against overlapping fields from SDSS DR8 (Aihara et al. 2011), yielding a global photometric accuracy and homogeneity of 2–3 percent over the whole survey area, which can be seen in Yuan et al. (in preparation).

Table 1 Fields Used for Extinction Coefficient Measurements and the Results

Date	Field [a]	Filter	k_1	k_2	k_c
2010/01/06	073824+2134	g	0.707 ± 0.010	-0.026 ± 0.001	0.028 ± 0.013
2010/01/14	073824+2134	g	0.739 ± 0.013	-0.028 ± 0.001	0.034 ± 0.007
	073824+2134[b]	g	0.649 ± 0.064	-0.107 ± 0.004	0.008 ± 0.000
2010/10/04	011800+3000	g	0.516 ± 0.017	-0.033 ± 0.001	0.036 ± 0.012
	011800+3000[b]	g	0.601 ± 0.022	-0.016 ± 0.003	0.022 ± 0.000
	202600+3000	g	0.761 ± 0.012	0.002 ± 0.001	-0.004 ± 0.000
2010/09/30	011800+3000	r	0.452 ± 0.008	-0.007 ± 0.001	0.012 ± 0.003
2010/10/05	011800+3000	r	0.649 ± 0.015	-0.017 ± 0.001	0.023 ± 0.003
	011800+3000[b]	r	0.399 ± 0.013	0.005 ± 0.002	-0.009 ± 0.002
	202600+3000	r	0.558 ± 0.013	-0.000 ± 0.001	0.009 ± 0.002
2010/01/13	073824+2134	i	0.383 ± 0.016	-0.000 ± 0.001	-0.004 ± 0.001

[a]: This column is a string expression of the field in a hhmmss+ddmm format.
[b]: The second observation of the same field on a descending path from the zenith.

3 ATMOSPHERIC EXTINCTION COEFFICIENTS

In the course of the XSTPS-GAC survey, six photometric nights were picked out in order to measure the atmospheric extinction coefficients – three nights for the g band, two nights for the r band and one night for the i band. In each night, repeated observations were carried out for one or two pre-selected fields, at different airmasses with intervals of about half an hour between the exposures. The observed fields for individual nights are listed in Table 1. In the current observations, given the large FoV of nearly 4 deg^2, thousands of bright, non-saturated stars with high signal-to-noise ratios as well as good astrometric calculations were captured in each of the individual exposure frames, and they can be utilized to determine the astrometric extinction coefficients. For this purpose, we need color information of individuals stars. As such, we choose our fields for atmospheric extinction measurements to overlap with SDSS stripes. The SDSS source catalogs, which go deeper than ours, then provide accurate colors for all stars utilized in the current work. Those colors are treated as "intrinsic" outside the Earth's atmosphere. However, note that there are some slight differences between the XSTPS-GAC and SDSS filters. Among the series of images taken for each of the fields, measurements made on one of the smallest airmasses were adopted as the references.

Individual frames were scrutinized and those that showed poor quality were rejected. Only isolated point sources within the central 1.0 deg^2 of the field and with good signal-to-noise ratios were selected. Specifically, we required that the stars should have SDSS r PSF magnitudes brighter than 17.0 mag and photometric errors less than 0.02 mag. In addition, the measurement uncertainties of the Xuyi photometry should also be less than 0.02 mag. The stars were then examined for potential variables. The observed magnitudes of individual stars at different values of airmass were plotted as a function of airmass, and sources possessing 3σ outliers with respect to a linear regression were rejected, as they were likely candidates of variable stars with large variations in amplitude.

Given the large FoV, the airmass of individual stars within the frame has to be calculated separately. In addition, the effect of the spherical Earth needs to be taken into account. The following formula of airmass given by Hardie & Ballard (1962) has been adopted

$$X = \sec z - 0.0018167(\sec z - 1) - 0.002875(\sec z - 1)^2 - 0.0008083(\sec z - 1)^3, \quad (1)$$

where z is the zenith angle in degrees. The zenith angle of individual stars can be calculated from their measured celestial coordinates, the observational UT time and date. Then the instrument magnitude of a star is linked to its "intrinsic" value at the smallest airmass by the relation,

$$m_{\rm inst} = m_0 + k_1 X + k_2 XC + k_c C + {\rm const}\,, \quad (2)$$

where $m_{\rm inst}$ is the stellar instrument magnitude, m_0 the instrument magnitude of the same star at the lowest airmass, k_1 the primary extinction coefficient, k_2 the second-order extinction coefficient that

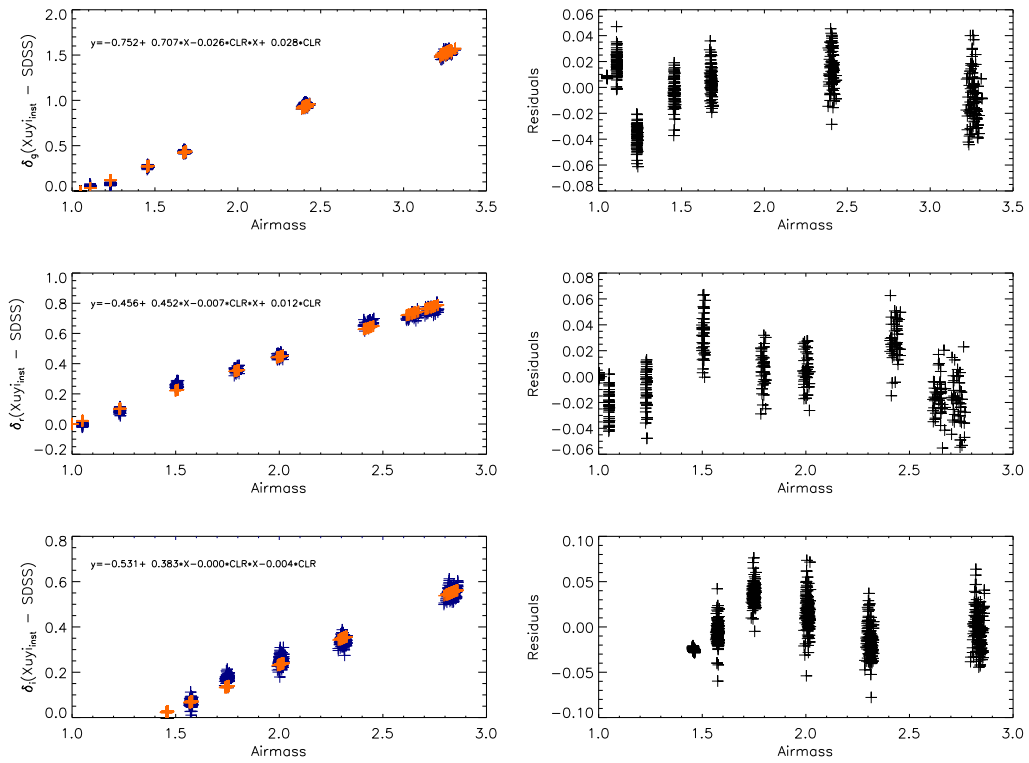

Fig. 1 The atmospheric extinction coefficients were estimated by fitting all data points from all usable stars in a given field as is illustrated here for g, r and i bands (*from top to bottom*), respectively. *Left*: The measured instrument magnitude relative to the SDSS measurements as a function of airmass, with observed values marked with blue color and fitted values marked with orange. *Right*: The residuals of the fit as a function of airmass.

is related to the color of the star, k_c a color correction factor that accounts for the small differences between the SDSS and Xuyi filter systems, C the intrinsic color of the star which is taken to be the $(g-i)$ value as given by the SDSS photometry here, and finally, 'const' a constant representing the zero point drift of the photometric system.

For each observed field, at least 50 stars are usable, with values of airmass for individual exposures spanning 1.0 to less larger than 3.0. The stars also span a wide range in color of more than 0.5 mag. Thus more than 50 equations in the form of Equation (2) could be constructed. Instead of resolving them individually, we fit all the data by a polynomial fitting in order to estimate the three extinction coefficients, k_1, k_2 and k_c. The results from individual fields are listed in Table 1.

Figure 1 shows three examples of the fitting results and their residual distribution for each band. From Table 1, we can see that the second extinction coefficient k_2 and the color coefficient k_c show some real variations with time and seem to need to be better constrained. The cause of the variations is probably related to the changes of observing conditions, such as the humidity, winds and so on. The primary extinction coefficients k_1 deduced for all three bands are large compared to typical values of some of the best astronomical sites (Mauna Kea, La Palama etc.), probably due to the low elevation of the Xuyi site. k_1 also shows large variations from night to night. It seems that k_1 becomes smaller after midnight, probably reflecting the drop of temperature and the content of

aerosols in the air. The average values of k_1 deduced from all observations are 0.69, 0.50 and 0.38 for the g, r and i bands, respectively. The i band coefficient is less well determined as there was only one night observation available. The relatively large value of the i band coefficient again possibly reflects the fact that aerosols are the dominant source of extinction for such a low altitude site.

There are three main sources of atmospheric extinction: the Rayleigh scattering, ozone absorption and aerosol dust extinction. Bessell (1990) provides an empirical formula to fit the extinction of each of the three components. The magnitudes of the Rayleigh scattering [$K_{\rm R} \propto \exp(-h_0/8)\lambda^{-4}$] and of the aerosol absorption [$K_{\rm A} \propto \exp(-h_0/1.5)\lambda^{-0.8}$] both depend on h_0, the altitude in km of the site above sea level. The low altitude of the Xuyi site is clearly the main reason for the relatively large extinction coefficients, especially that of the g band, compared to other good astronomical sites which are generally at much higher altitudes. Given the significant variations of the extinction coefficients from night to night, some care must be exercised if one uses the average values presented here to reduce the whole data.

4 NIGHT SKY BRIGHTNESS

The sources contributing to night sky brightness include diffuse stellar light scattered by the interstellar medium, solar and lunar light scattered by atmospheric dust grains, faint unresolved stars and galaxies within the field of view, and scattered artificial light of nearby cities. La Palma technical note 115 summarized the contributions of individual sources to the night sky brightness at that site (*http://www.ing.iac.es/Astronomy/observing/conditions/skybr/skybr.html*). We refer the reader to this work for details on the origins and contributions of various light sources and their potential effects on observations of different types of targets. In this work, we measure the night sky brightness of the Xuyi site.

4.1 Methods

The Xuyi site is just about a hundred kilometers away from Nanjing city and Huai'an city, and is several tens of kilometers away from the nearest Xuyi town. This could be seen on the map of the East Asia artificial night light picture from NASA's "Blue Marble" project (2010 version), with a small part near the observation site cut out and shown in the left panel of Figure 2. The artificial light pollution from the nearby cities and towns is clearly visible and poses a danger to the site. On photometric nights, the light pollution is less of a problem, but on partially cloudy nights, even the slightest light pollution may cause a big problem for astronomical observations due to the effects of scattering.

Only good quality images collected in the XSTPS-GAC survey have been used to measure the night sky brightness. Images collected under cloudy conditions can be easily rejected from their abnormally bright background. To the limiting magnitude of the survey, even for crowded fields near the Galactic plane, only a small fraction of pixels are on stars or galaxies, while the rest fall on blank sky. Thus, after clipping bright pixels of stars and galaxies, the median count of blank pixels within the central 1024×1024 CCD chip, denoted by $\rm sky_{count}$, serves as a robust measurement of the sky background. Then, the sky instrument brightness $\rm sky_{inst}$ of a given image is calculated using

$$\rm sky_{inst} = 25.0 - 2.5 \times \log_{10}(sky_{count}/scale^2), \tag{3}$$

where 'scale' is the angular size of a CCD pixel projected on the sky, i.e. $1.705''$ in this work.

Then the sky brightness $\rm sky_B$, in units of mag arcsec^{-2}, can be calculated by:

$$\rm sky_B = sky_{inst} + \mathit{zp}, \tag{4}$$

$$\mathit{zp} = \delta + \rm ext + \mathit{c_c}, \tag{5}$$

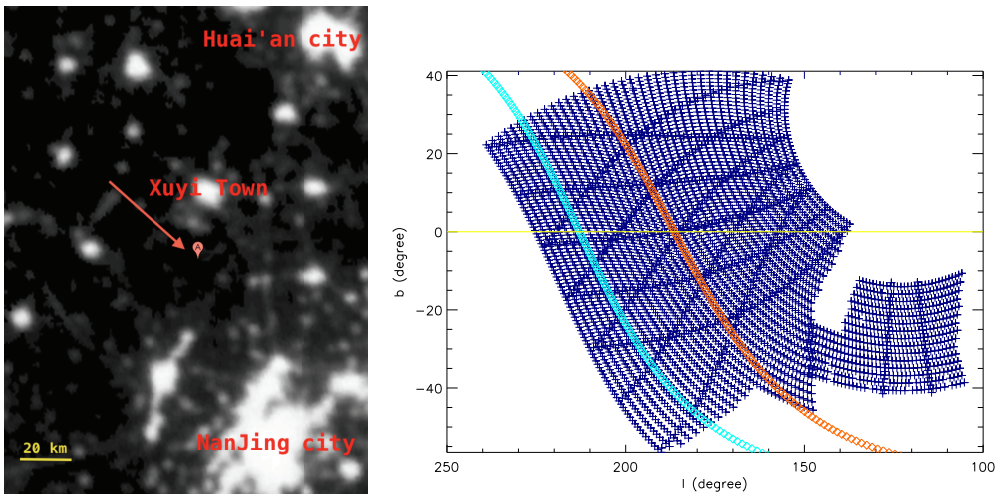

Fig. 2 *Left*: A small portion of the map of the artificial night light from NASA's "Blue Marble" pictures (*http://www.blue-marble.de/*; 2010 version), centered on the Xuyi site, marked by an arrow. The large patches of heavy light pollution are marked: the one near the bottom is Nanjing city and the one near the top is Huai'an city. The approximate scale is labeled in the left-corner. *Right*: The sky coverage of XSTPS-GAC fields. The yellow line denotes the Galactic plane, whereas the orange and blue diamonds denote the ecliptic and celestial equators, respectively.

where zp is the instrument zero point, 'ext' is the atmospheric extinction which adopted the same values as deduced in the previous section, C_c is the color correction factor and δ is the zero point for the image. Values of δ in this work are from Yuan et al. (in preparation). Here the intrinsic night sky brightness out of the atmosphere is calculated, and we find a significant fraction of the night sky brightness at the Xuyi site is from light pollution, as shown later.

4.2 Discussion

The right panel of Figure 2 shows that XSTPS-GAC covers the Galactic disk and the ecliptic, so the data can be used to study the effects of the Galactic disk and zodiacal light on the night sky brightness. Similarly, we can study the dependence of the sky brightness on the solar cycle as well as the lunar phase. The lunar phase P is normalized to 0–15, where 0 represents the new Moon and 15 the full Moon.

The XSTPS-GAC was carried out during the early phase of the 24th solar cycle, from October 2009 to March 2012. The level of solar activity was normal and the data showed no obvious evidence that the night sky brightness was affected by solar activities. This also implies that some caution must be taken when comparing measurements of the night sky brightness presented in the current work to other years with higher levels of solar activity.

To minimize the effects of the bright Galactic disk, we calculated the night sky brightness for each band using images of ecliptic latitudes $|\beta| > 20^\circ$ and Galactic latitudes $|b| > 15^\circ$, taken under lunar phases < 7, lunar angular distances $> 90^\circ$ and lunar altitude $< 0^\circ$.

Figure 3 shows the histograms of the night sky brightness distribution that were deduced for the g, r and i bands. The median values of the night sky brightness were $g = 21.7$, $r = 20.8$ and $i = 20.0$ mag arcsec^{-2}. Figure 3 also shows that under the best observing conditions, the night sky brightness can be as faint as 22.1, 21.2 and 20.4 mag arcsec^{-2} in the g, r and i bands,

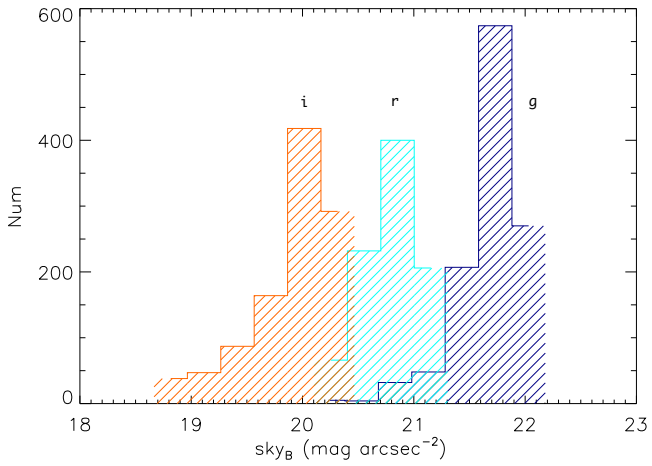

Fig. 3 Histograms of the night sky brightness in g (*blue*), r (*cyan*) and i (*orange*) bands, deduced from images of Galactic latitudes $|b| > 15°$, and taken under lunar phases < 7 and angular distances $> 90°$. More details can be seen in the text.

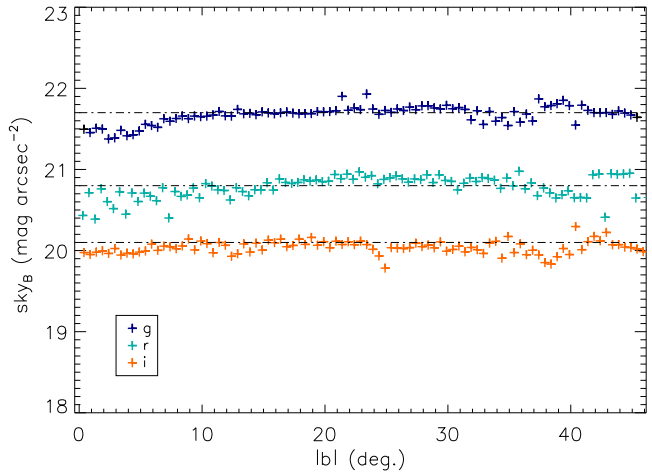

Fig. 4 Variations in the night sky brightness as a function of Galactic latitude. The dot-dashed lines represent the median values adopted for the Xuyi site. Each plus symbol represents the median sky brightness with a binsize of 0.5 °, in units of mag arcsec^{-2}.

respectively. Based on the transformation equations for Population I stars between SDSS magnitudes and $UBVR_CI_C$ given by Jordi et al. (2006)

$$V - g = (-0.573 \pm 0.002) \times (g - r) - (0.016 \pm 0.002) \quad (6)$$

and adopting $g - r = 0.8$ as the color of the night sky, we find that a typical value of night sky brightness in the V band is $V = 21.2$ mag arcsec^{-2}, which is very close to that of the Xinglong Station (Yao et al. 2012), but can reach $V = 21.6$ mag arcsec^{-2} under the best conditions. Note that

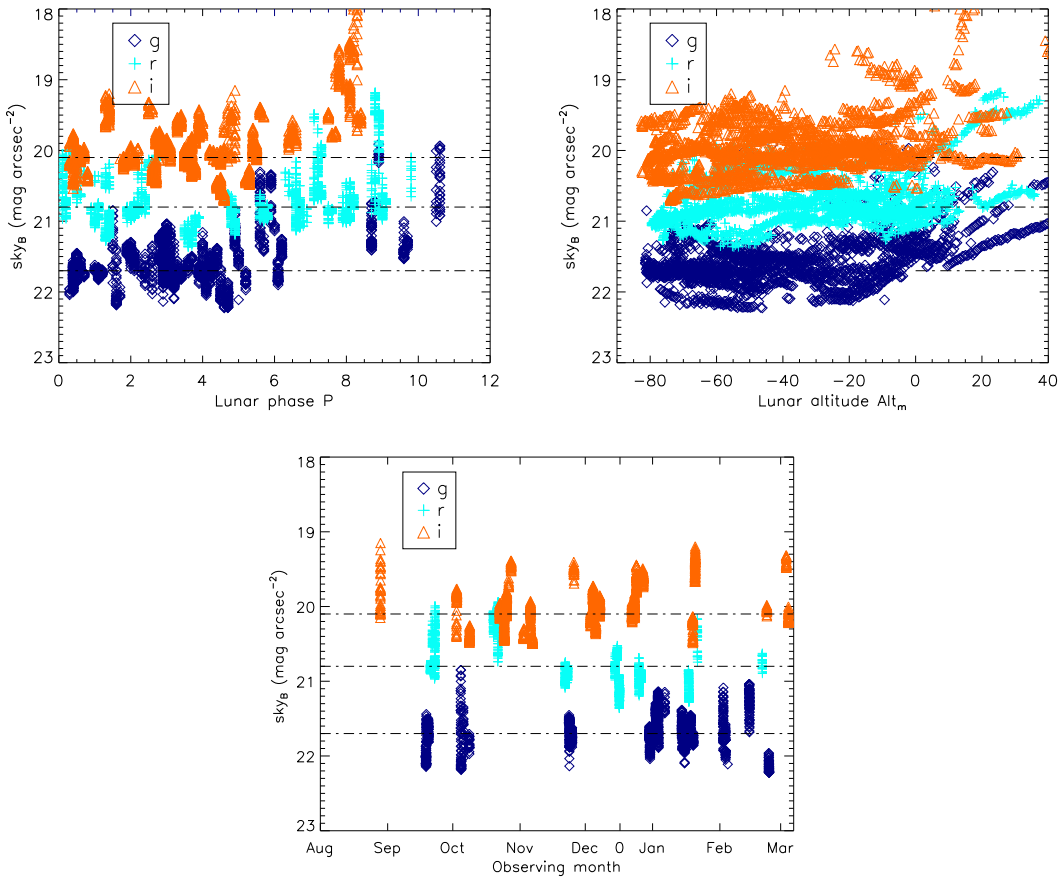

Fig. 5 Variations of the night sky brightness with lunar phase P (*top-left*) and altitude $\mathrm{alt_m}$ (*top-right*). In the bottom panel, only data points with $P < 6$ and $\mathrm{alt_m} < 0$ are shown. The color codes of the data points are the same as those in Fig. 3.

the night sky brightness at world-class sites can reach a typical value of $V = 21.9$ mag arcsec^{-2} (Benn & Ellison 1998), suggesting that a significant fraction of the night sky brightness at the Xuyi site is from light pollution.

To investigate the effect of diffuse light from the Galactic disk, night sky brightness values deduced from images of ecliptic latitudes $|\beta| > 15°$, secured under lunar phases $P < 7$, lunar altitudes $< 0°$ and lunar angular distances $> 90°$, are plotted against Galactic latitudes in Figure 4. Even though there are some fluctuations, we can see that the Galactic disk enhances the night sky by about 0.3 and 0.2 mag arcsec^{-2} in the g and r bands, respectively. However, the effect in the i band is not obvious. Similarly, images of Galactic latitudes $|b| > 10°$, obtained under lunar phases $P < 7$, lunar altitudes < 0 and lunar angle distances $> 90°$, were used to study the variations of night sky brightness with ecliptic latitude. No obvious variations of the night sky brightness with ecliptic latitude are found in any of the three bands.

Finally, we study the dependence of night sky brightness on the lunar phase P, lunar altitude $\mathrm{alt_m}$, and the angular distance D between the field center and the Moon. A similar work on the effects of the Moon on the night sky brightness is presented by Krisciunas & Schaefer (1991). Note

all the observations were taken under lunar phase $P < 10$. Our results are shown in Figure 5. The top left panel of Figure 5 shows that the night sky brightness is nearly flat for $P < 6$, but increases significantly thereafter at a rate of about 0.3, 0.2 and 0.2 mag arcsec^{-2} per night for the g, r and i bands, respectively. The night sky brightness is also found to be nearly constant for lunar altitudes smaller than 0°, i.e. below the horizon, and then brightens by about 0.2, 0.1 and 0.1 mag arcsec^{-2} every 10 ° for the three bands respectively as the Moon rises. The bottom panel of Figure 5 shows the seasonal variations of the night sky brightness; only images of $P < 6$ and alt$_{\rm m} < 0$ were used. No clear seasonal variations are seen in the three bands.

5 CONCLUSIONS

In this work, we present measurements of the optical broadband atmospheric extinction coefficients and the night sky brightness at the Purple Mountain Observatory's Xuyi site, based on the large data set collected for the XSTPS-GAC survey from 2009 to 2011. The mean extinction coefficients are 0.69, 0.55 and 0.38 mag/airmass for the g, r and i bands, respectively. The values are larger than the best astronomical sites around the world, and with some variations from night to night. So, this result represents the typical atmospheric extinction for the site. Thus, it is unwise to use a single mean extinction coefficient to do the flux calibration for the whole data, which will introduce large errors.

The typical night sky brightness is 21.7, 20.8 and 20.0 mag arcsec^{-2} in the g, r and i bands, respectively, which corresponds to $V = 21.2$ mag. The night sky brightness could reach as faint as 22.1, 21.2 and 20.4 mag arcsec^{-2} under the best conditions. A significant fraction of night sky brightness is from light pollution. The diffuse light from the Galactic disk enhances the night sky brightness by about 0.3, 0.2 and 0.2 mag arcsec^{-2} in the g, r and i bands, respectively. But the zodiacal light has almost no obvious influence. There are no variations if lunar phase $P < 6$ and lunar altitudes alt$_m < 0$. The night sky brightness will be respectively brightened by about 0.3, 0.2 and 0.2 mag per night after lunar phase $P > 7$ and 0.02, 0.01 and 0.01 mag per degree with lunar altitudes alt$_{\rm m}$ above the horizon. The relatively faint night sky brightness makes it a good observational site in China for wide field surveys. To protect the site from further deterioration, light pollution must be strictly controlled for any resort development around the area.

Acknowledgements This work is supported by the National Natural Science Foundation of China (Grant Nos. 11078006 and 10933004). This work is also supported by the Minor Planet Foundation of Purple Mountain Observatory.

References

Aihara, H., Allende Prieto, C., An, D., et al. 2011, ApJS, 193, 29
Benn, C. S., & Ellison, S. L. 1998, New Astronomy Reviews, 42, 503
Bessell, M. S. 1990, PASP, 102, 1181
Bucciarelli, B., García Yus, J., Casalegno, R., et al. 2001, A&A, 368, 335
Burke, D. L., Axelrod, T., Blondin, S., et al. 2010, ApJ, 720, 811
Burki, G., Rufener, F., Burnet, M., et al. 1995, A&AS, 112, 383
Fan, X., Burstein, D., Chen, J.-S., et al. 1996, AJ, 112, 628
García-Gil, A., Muñoz-Tuñón, C., & Varela, A. M. 2010, PASP, 122, 1109
Garstang, R. H. 1989, PASP, 101, 306
Hampf, D., Rowell, G., Wild, N., et al. 2011, Advances in Space Research, 48, 1017
Hardie, R. H., & Ballard, C. M. 1962, PASP, 74, 242
Hogg, D. W., Finkbeiner, D. P., Schlegel, D. J., & Gunn, J. E. 2001, AJ, 122, 2129
Jordi, K., Grebel, E. K., & Ammon, K. 2006, A&A, 460, 339

Krisciunas, K. 1990, PASP, 102, 1052
Krisciunas, K. 1997, PASP, 109, 1181
Krisciunas, K., & Schaefer, B. E. 1991, PASP, 103, 1033
Krisciunas, K., Sinton, W., Tholen, K., et al. 1987, PASP, 99, 887
Liu, Y., Zhou, X., Sun, W.-H., et al. 2003, PASP, 115, 495
Mattila, K., Vaeisaenen, P., & Appen-Schnur, G. F. O. V. 1996, A&AS, 119, 153
Padmanabhan, N., Schlegel, D. J., Finkbeiner, D. P., et al. 2008, ApJ, 674, 1217
Parrao, L., & Schuster, W. J. 2003, in Revista Mexicana de Astronomia y Astrofisica Conference Series, 19, eds. I. Cruz-Gonzalez, R. Avila, & M. Tapia, 81
Patat, F., Moehler, S., O'Brien, K., et al. 2011, A&A, 527, A91
Roeser, S., Demleitner, M., & Schilbach, E. 2010, AJ, 139, 2440
Stetson, P. B. 1987, PASP, 99, 191
Tokovinin, A., & Travouillon, T. 2006, MNRAS, 365, 1235
Yan, H., Burstein, D., Fan, X., et al. 2000, PASP, 112, 691
Yao, S., Liu, C., Zhang, H.-T., et al. 2012, RAA (Research in Astronomy and Astrophysics), 12, 772
Zhou, X., Jiang, Z.-J., Xue, S.-J., et al. 2001, ChJAA (Chin. J. Astron. Astrophys.), 1, 372